INVITED PAPER

Framework for the Development of Neuroprostheses: From Basic Understanding by Sciatic and Median Nerves Models to Bionic Legs and Hands

This paper focuses on a novel, less invasive or intrusive neural prosthesis design by optimizing the neural interface geometry and the number of stimulating contacts for any specific nerve.

By Stanisa Raspopovic, Francesco Maria Petrini, Marek Zelechowski, and Giacomo Valle

ABSTRACT | Neuroprostheses based on electrical stimulation are becoming a therapeutic reality, dramatically improving the life of disabled people. They are based on neural interfaces that are designed to create an intimate contact with neural cells. These devices speak the language of electron currents, while the human nervous system uses ionic currents to communicate. A deep understanding of the complex interplay between these currents, during the electrical stimulation, is essential for the development of optimized neuroprostheses. Neural electrodes can have different geometries, placement within the nervous system, and the stimulation protocols (paradigms of use). This high-dimensional problem is not tractable by an empiric, brute-force approach and should be tackled by exact computational models, making use of our accumulated knowledge. In pursuit of this goal, a hybrid finite element method–NEURON modeling–is used for a solution of electrical field generated by stimulation, within the different neural structures having anisotropic conductivity, and a corresponding neural response computation. In this work, an important correction of perineurium electrical conductivity is computed. Models of median and sciatic nerves, innervating the hand and foot areas, relevant to the development of bionic hands and legs with sensory feedback, are implemented. The obtained results have the potential to optimize the design of neural interfaces, in terms of shape and number of stimulating contacts. Guidelines for the neurosurgical planning are proposed, by indicating the optimal number of implants for a specific nerve to obtain the best efficacy with the lowest invasiveness. The interpretation is proposed for one of the basic problems of neural interfaces, consisting in the change of the stimulation threshold due to fibrotic reaction of tissue. We show that it is possible to use human microstimulation as an experimental setup for testing of afferent stimulation paradigms, which can be translated to further chronic implants. In the future, models will have a key role in the decision of the most appropriate design of customized neuroprostheses, their optimal modality of use,

Manuscript received March 31, 2016; revised July 1, 2016; accepted August 4, 2016. Date of publication September 16, 2016; date of current version December 20, 2016. This work was supported in part by the European Union under Grants FP7-602547 EPIONE and FP7-611687 NEBIAS.

The authors are with the Translational Neural Engineering Laboratory, School of Engineering, Ecole Polytechnique Federale de Lausanne, and Center for Neuroprosthetics and Institute of Bioengineering, School of Engineering, 1015 Lausanne, Switzerland (e-mail: stanisa.raspopovic@epfl.ch; francesco.petrini86@gmail.com; marek.zelechowski@gmail.com; vallegiacomo@gmail.com).

Digital Object Identifier: 10.1109/JPROC.2016.2600560

understanding the effects that occur during their use, and minimizing animal and human experimentation.

KEYWORDS | Computational model; electrical peripheral nerve stimulation; finite element model; NEURON model; prosthesis; sensory feedback

I. INTRODUCTION

Neuroprostheses are becoming widespread therapeutic solutions, targeting human nervous system at different levels. These devices can significantly improve the quality of life of people who have suffered from neurological disabilities.

They have shown their beneficial effects in the treatment of Parkinson disease, by means of deep brain stimulation (DBS) [1], certain type of blindness by retinal implants [2], deafness by cochlear stimulation [3], walking rehabilitation in spinal cord injured (SCI) patients by epidural stimulation [4], pain suppression by spinal stimulation [5], and recently for the restoration of sensory feedback in bidirectional upper limb prostheses [6], [7].

At first, research efforts were oriented to understand the biocompatibility and basic functionality [8], [9] of the proposed devices, however, the need for an exhaustive understanding of the interaction between implanted electrodes and the response of the neural tissue became evident [10]. This is due to the fact that neuroprostheses can stimulate by a range of different values for frequency, pulse width and amplitude, delivered through multiple active sites (ASs), located in various positions within the nervous system [11]. The proper selection of all these parameters contributes to a success of a neuroprosthetic device, and this high-dimensional problem is difficult to address by using empirical, experiment-based knowledge. Instead, computational models, being founded on precise physical knowledge of the problem, are better candidates to address the aforementioned questions.

One of the first analytical models, explaining the influence of external electrical fields on the myelinated axons, was proposed by McNeal [12], resulting in the concept of so-called "activating function" (AF). This work exploited the fact that, although neural devices and neurons have different communicating currents, they share the same electric field. Electric field is modulated by injected electrical currents, and can depolarize the external membrane of neurons, causing the ionic currents flow, which can trigger the spikes, the basic carriers of information in the human nervous system. Through the AF, McNeal proposed that the likelihood of neuronal activation due to an external electrical stimulation is proportional to the second derivative of the external voltage field with respect to neuronal spatial extension. Rattay [13], [14] extended this concept by generalizing it to include unmyelinated axons, and realistic electrode-like current sources, instead of point sources.

Even though the AF is still used as the most rapid and intuitive indicator to estimate axonal responses to electrical stimuli, recent studies [15], [16] have shown that it introduces important errors. The main reasons for these errors were that the AF approach neglects the high nonlinearity of axonal responses and the anisotropy of the medium in which the neurons are inserted.

In contrast to the AF approach, modern computational models [17]–[26] account for both the anisotropic extracellular conductivity of real nerves, and for the dynamic response of neuronal cells and axons to the extracellular electrical stimulation. In order to calculate the voltages induced by electrical stimuli injected through an electrode into the anisotropic medium, the finite element method (FEM) is exploited. The axonal responses to these voltages can then be calculated by using specific software for efficient calculus of neuronal dynamic (NEURON [27]). The results of FEM are interpolated into the NEURON model, obtaining a "hybrid electro-neuronal model." The initial concept of hybrid modeling was proposed in the works related with the electrical epidural stimulation (EES) of spinal cord [28], [29]. Subsequently, a similar framework has been exploited in works that model extracellular stimulation of central nervous system neurons, in particular, for DBS [20], [21]. Recently, it has been applied to the human peripheral nervous system to optimize the design of extraneural cuff electrodes [18] for motor rehabilitation of SCI patients. Intraneural electrodes as interface with the peripheral nerve have been simulated [19] and the model has been validated [30] in rat implants, using the same hybrid modeling approach. Successful clinical translational use of models in the CNS culminated in the development of software like CICERONE [21], which is used in DBS therapy preparation, or in software for simulating the spinal cord stimulation [22]. This, in turn, led to the development of sophisticated stimulation paradigms, which enabled an unseen level of mobility in fully SCI rats. These models were not only important from the translational viewpoint, by indicating the best electrodes placement and principles for the optimal stimulation, but also enabled a more in-depth understanding of several mechanisms. Indeed, computer simulations [23]–[25] provided evidence that EES primarily engages large myelinated fibers associated with proprioceptive and cutaneous feedback circuits during the SCI rehabilitation. The pivotal role played by models in all these complex systems solicits the need for the implementation of similar realistic ones also for the human PNS, to be exploited within the development of a bionic prostheses with sensory feedback [6], [7]. Neural interfaces are an important component of these systems: they allow a direct contact with the nerves. Several neural interfaces for the PNS have been developed during the past years. Epineural

electrodes, constituted by an insulating substrate with ASs placed around the nerve (e.g., spiral cuff [31], or flat interface nerve electrode (FINE) [7]) are characterized by low invasiveness and low selectivity. Regenerative electrodes, which guide the regrowth of transected nerves, through their ASs, are characterized by high selectivity at price of high invasiveness [8]. A good tradeoff between the two previous solutions can be found in intraneural interfaces, such as the transverse intrafascicular multichannel electrode (TIME) [32], or SELINE electrodes [33], both consisting of a polyimide substrate with ASs on both sides.

This work shows the use of models of human median [34] and sciatic nerves electrical stimulation (ePNS) within the framework of development of innovative neuroprostheses (Fig. 1). The median nerve innervates the major part of hand sensory area and, therefore, is essential for the bidirectional control during objects manipulation. The sciatic nerve innervates almost the whole foot sole, having a crucial role for the human balance and walking ability. Restoration of natural sensations from missing hand and foot will enable correct sensory-motor integration of prosthetic devices by reintroducing the brain into the loop, and thereby will substantially improve the recovery of disabled people.

The efficacy of neuroprostheses can be improved by increasing the selectivity of neural interfaces, which is the capability to stimulate only specific subsets of cells while not soliciting untargeted ones. It is also beneficial to diminish their invasiveness (dimensions) and reduce the amount of current to be injected into the tissues. Indeed, selectivity is strongly influenced by the interface design, particularly by dimensions of the whole device, its shape, number, and interdistance between active

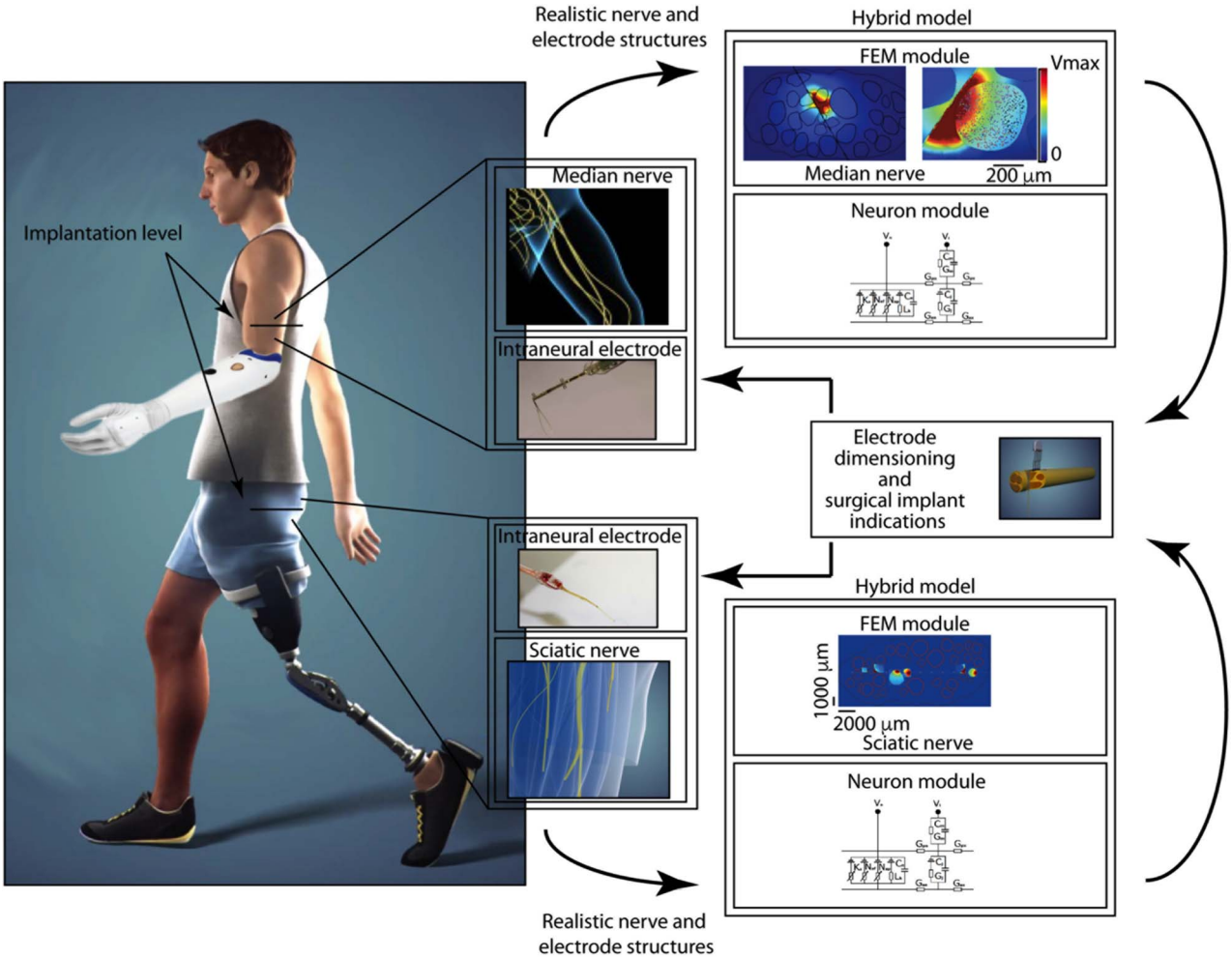

Fig. 1. ***Hybrid modeling framework for the development of optimal prostheses with sensory feedback for hand and leg: median and sciatic nerves sections are taken at the appropriate level for the implantation, and then used, within the hybrid electroneuronal models for the development of the optimized neural interfaces for selective and minimally invasive use. Represented intraneural electrodes are TIME [32] and SELINE [33].***

contacts used for tissue stimulation. Moreover, models can indicate the optimal number of devices to be implanted within the single nerve, and therefore can give valuable indications on how the neurosurgery should be performed. Generally, the neural interfaces were tested *in vitro* or in animal preparation by single-channel stimulation and measurements of several output parameters, like muscle recruitment curves [35]. Unfortunately, this strategy does not exploit optimally the capabilities offered by implanted devices, and in particular does not allow to address subject-specific deficits, so as to maximize the outcome of rehabilitation protocols. Since the use of more sophisticated stimulation paradigms has shown interesting results [36]–[39], new strategies (e.g., evocation of more natural sensations in amputees [7] and the combinations of several ASs [40]) should be extensively explored.

One of the biggest problems encountered during the use of neural interfaces that lacks of a proper interpretation is the change over time of the charge necessary (threshold) to elicit perceivable sensations [6], [7]. This is most probably due to the complex tissue reaction: some aspects of this issue can be explained by using models, rather than sacrificing an extensive number of animals followed by histological analysis [9], [41]–[44]. The development of prostheses with sensory feedback suffers from difficult animal validation, since animals cannot describe their perceptions.

The use of minimally invasive human microneurography is potentially the method for experimental testing of sensory stimulations paradigms, which can be translated to chronic implants. We used a model to explore that possibility.

Moreover, in the following sections, we will illustrate how hybrid models for sciatic and median nerves are developed, how they can guide us toward an optimal design and innovative use of electrodes, and give an insight about a possible interpretation of threshold changes during the prolonged use of neuroprostheses.

II. FRAMEWORK FOR THE DEVELOPMENT OF THE HYBRID MODEL

Here we formulate a three-step framework for the development of the hybrid electroneural model. A realistic FEM model is developed taking into account the anatomical and physiological features of human nerves. Electric potentials are calculated, and interpolated voltages are applied to the compartmental models of human tactile fibers, implemented on the base of experimental biophysical data.

A. Finite Elements Model

We implemented anatomically realistic finite element volume conductor models of the human sciatic and median nerves (see Fig. 1). To achieve this, we first identified the histological section images at the appropriate nerves level, where the electrodes are implanted. In the case of the median nerve, the implant height is above the elbow [45], since we are considering prostheses for transradial (under-elbow) amputees. In the case of the sciatic nerve implant, the chosen level corresponds to the ischial tuberosity [46], since it should be available for all transfemoral (thigh-level) amputees. Then, the images are segmented by means of specialized algorithms (ImageJ: http://rsb.info-nih.gov/ij), obtaining anatomically shaped geometrical models. Afterwards, the segmented geometry is imported into the FEM software, COMSOL (COMSOL S.r.l., Italy) and extruded along the longitudinal axis achieving a 3-D structure (see Fig. 2).

A crucial aspect is the correct assignment of the different tissue classes (epineurium, perineurium, and endoneurium) with their specific electrical properties. These values are available in literature, however they need to be critically inspected, and adapted. The intrafascicular endoneurium, due to the longitudinal disposal of axon within it, has an anisotropic conductivity tensor with a longitudinal value of 0.571 S/m and a transverse value of 0.0826 S/m [18], [19]. The epineurium is assumed to be an isotropic medium with a conductivity of 0.0826 S/m [18], [19]. The perineurium is generally modeled as an isotropic conductor according to [47],

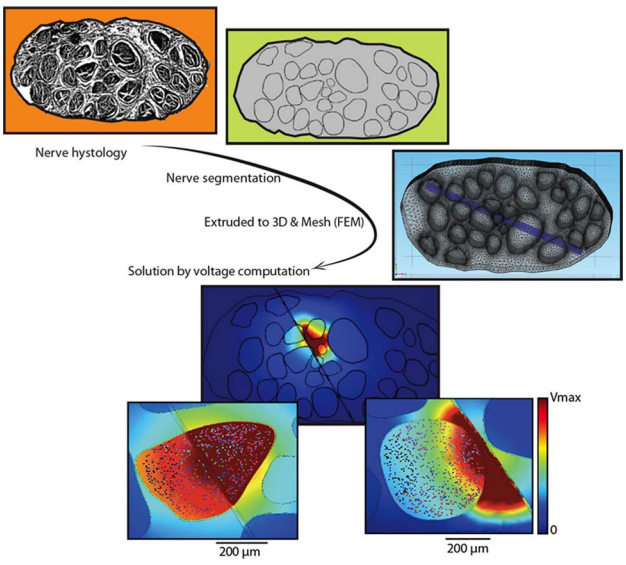

Fig. 2. *FE model construction and solution: the histological section is taken at the nerve's level of interest (indicated in Fig. 1. for sciatic and median nerve). Then, the segmentation of the image is performed, and different structures (endoneurium, perineurium, epineurium) are electrically characterized. Electrode is merged, and overall FEM is meshed. Finally, the solution is computed, solving the Laplace equation by means of the numerical solver. In the last row, the voltages elicited by two different electrode ASs and the positions of implemented axons are depicted.*

[48] with a value of 0.0021 S/m, but in this work, this value has been corrected, as detailed in Section II-A1. The nerves surroundings are implemented as a homogeneous saline solution cylinder (2 S/m), which emulates the intraoperative environment. Models of electrodes are constructed separately and merged with the neural structure. Since the frequency range of interest for our applications is low, a quasi-static approximation of Maxwell's equations within the nerve volume can be assumed [49]. Therefore, the electromagnetic problem can be expressed through Laplace formulation for the extracellular electric potential [17]:

$$\nabla \cdot \sigma \nabla V_e = 0. \tag{1}$$

This is solved by numerical methods, where the discretization is performed by the operation of mesh formation [10], [17], [19]. The development of models for intraneural electrodes is particularly challenging because they are located within the neural structures, leading to computationally intensive meshing tasks. In particular, for median and sciatic nerves, a nonuniform mesh of tetrahedral and cubic elements was used. Higher elements' density is used in proximity of the electrode, where the induced electric field gradient is higher, and therefore fine details are needed (see Fig. 2) [10], [17], [19].

1) Determination of Electrical Parameters: Correction of the Perineurium Conductivity: One of the most important electrical values to consider, during the model implementation, is the perineurium conductivity. This thin structure, due to its high resistivity, acts as a strong insulator to the current flow. The value of conductivity of the perineurium is often taken from [18], [47], and [48], which extrapolate it from frog values [50], assuming perineurium thickness of 100 μm [47]. We recalculated this value taking into account the thickness of the perineurium as 3% of the approximate diameter of the fascicle, as proposed in [51], and the difference of temperature between frogs and humans. In frog experiments, an average sheet resistance value of 478 $\Omega \cdot$ cm2 [50] is reported. In that study, 725 μm was the average value for the diameter of the fascicles. Dividing the sheet resistance by the derived average thickness of perineurium (3% of 725 results in 22 μm) yields a perineurium resistivity of $2.178 * 105\ \Omega$, which results in the frog conductivity at 21 °C of:

$$\sigma_{s,21\,^\circ\mathrm{C}} = 4.6 \cdot 10^{-4}\ \mathrm{S/m}. \tag{2}$$

Consequently, by using [52], we extrapolate the conductivity at 37 °C (human):

$$\sigma_{s,37\,^\circ\mathrm{C}} = \sigma_{s,21\,^\circ\mathrm{C}} \cdot Q_{10}^{\frac{(37-21)}{10}}$$
$$\text{Assuming } Q_{10} = 1.5 \text{ it results in :}$$
$$\sigma_{\text{perineurium}} = 0.00088\ \mathrm{S/m}. \tag{3}$$

It is a significant change with respect to the generally used value of 0.021 S/m [18], [47], [48].

2) Determination of the Correct Boundary Conditions: While in physics the 0-voltage is defined at infinity, within the FEM model, to emulate the proper boundary conditions of the problem, the ground condition is set to the outermost surface of a finite model [17]. Clearly, an error in the electromagnetic solution is introduced when approximating an infinite-length/infinite-diameter structure with a finite-length/finite-diameter saline solution. A tradeoff has to be made regarding the size of the model: the goal is to minimize the error to a sufficiently small level within the constraints of available computational resources.

To find the optimal boundaries, a set of appropriate indexes (Table 1) is defined [19]. The correlation coefficient illustrates a statistical relationship of variables or data. In this case, values of the coefficient ranging from 0 to 1 determine a measure for topological differences of two electric potential maps. The magnification factor [48] is used to measure the relative magnitude between two potential distributions and the root-mean-square error is a commonly used measure of difference of two variables. Similar indexes are often used for FEM electromagnetic problems related to EEG source imaging [53], where different electric potential maps over the scalp surface must be compared.

Operatively, several models with external saline cylinders of different lengths and widths are solved. The computed electric potentials (volts) are evaluated over surfaces in the parallel transverse planes. The computation surfaces are located along the nerve length at distances corresponding to, or smaller than, the one between two Ranvier nodes. They are taken, starting from the plane ($z = 0$), crossing the center of stimulating ASs, up to 10 mm in both directions from it, which correspond approximately to the location of the last modeled nodes. Then, the indexes (Table 1) are computed over these voltages.

When the indexes, calculated for different dimensions, do not change with model's dimension increase, the model itself results in the minimal acceptable correct boundary conditions, and is computationally the most efficient to exploit.

B. Neuron Compartmental Models

The difference among state-of-the-art models basically resides in two aspects: the first is the membrane dynamics and the second is the representation of the neuron compartments (Ranvier nodes and axon tracts between them). Membrane dynamics refers to the differential equations characterizing the membrane and extracellular potentials (i.e., the number of ion channels implemented), while compartment representations refer to the number and type of compartments (see Fig. 3). To

Table 1 Indexes to Compute for Correct Boundaries Definition. Defined in [19]

Index	Definition
Correlation Coefficient	$CC = \frac{\sum_{i=1}^{N}(V_i^1 - \bar{V}^1)(V_i^2 - \bar{V}^2)}{\sqrt{\sum_{i=1}^{N}(V_i^1 - \bar{V}^1)^2}\sqrt{\sum_{i=1}^{N}(V_i^2 - \bar{V}^2)^2}}$
Magnification factor	$MAG = \frac{\sqrt{\sum_{i=1}^{N}(V_i^1)^2}}{\sqrt{\sum_{i=1}^{N}(V_i^2)^2}}$
Root Mean Square Error	$RMSE = \sqrt{\frac{1}{N}\sum_{i=1}^{N}(V_i^1 - V_i^2)^2}$

represent the dynamics of a nerve fiber, a McIntyre–Richardson–Grill (MRG) model was used [26]. This model represents the nonlinear modified Hodgkin–Huxley equations [54] for the active compartment of the axons (the nodes of Ranvier) and a detailed realistic representation of the myelinated tracts [see Fig. 3(b)].

The sensory axon populations were simulated in NEURON 7.3. In particular, a fiber of diameter D, made of 21 nodes of Ranvier, with an internodal space $L = 100 * D$, was built, and NEURON's extracellular stimulation procedure was used to excite the cell.

It is unknown where the fibers' groups, which convey a specific sensation, are placed: they either spread over the whole fascicle, or only within a very limited area. Moreover, fibers vary in diameter. To address these issues, 100 fibers were positioned in each targeted fascicle, and they were randomly displaced generating several possible populations to contemplate anatomical variability [Fig. 3(a)]. Specifically, depending on the fascicle size, between 1 and 9 populations were created, each containing the same number of fibers, and located in different portions of the fascicle. In order to implement the populations of sensory axons for the median nerve, we used [55] and [56], which explored the functional properties of human hand tactile units, by microneurographic recordings. Starting from their findings, we modeled the probabilistic distribution of the fibers diameter as two Gaussian distributions, which differentiated nociceptive fibers from those responsible for pressure/touch sensation. The nodal length was fixed at 1 μm and the nodal diameter was scaled as in [26]. Three groups of fascicles, representing three different sizes, were taken into account for the following analyses: small (one population implemented), medium (five populations), and large (nine populations). Finally, we assumed that fibers within a specific fascicle innervate the same portion of the hand [45].

For the sciatic nerve, the steps described in the case of the median nerve model were reproduced, and similar assumptions were made (neighboring fibers innervate the same portion of the foot). The fiber diameter distribution was generated from data gathered in [57]–[59]. Specifically for the sciatic nerve, depending on the fascicles size, between 1 and 5 fibers populations were created, each including diameters and dynamics of the foot tactile units [57]–[59]. A fascicle was considered small when its approximated diameter did not exceed 400 μm and within it, one fiber population was implemented. A medium fascicle diameter ranged from 400 to 800 μm, and had three populations, while the large one contained five simulated populations.

C. Merging of FEM and NEURON: Hybrid Model

Electric potentials generated inside the nerve by means of electrical stimulation were computed for the whole structure. Then, they were interpolated on the proper fiber positions and then the neurons' response was computed accordingly (see Fig. 4). As the positioning of the nodes of Ranvier is stochastic with respect to the central orthogonal plane of the model, a random shift of the nodes from $-L/2$, to $+L/2$ along the longitudinal direction, where L represents the intranodal distance (paranodal length), was implemented. Electric potentials were then interpolated on the position of the nodes of Ranvier and on the paranode positions, for each fiber implemented in NEURON, and exploited as an extracellular mechanism [27] for membrane depolarization. A fiber was considered recruited when a generated action potential traveled along its whole length (i.e., reached the last node of Ranvier). Electrical stimulation was implemented like cathodic first, bipolar, rectangular current pulses [11]. During simulation we varied pulsewidth and amplitude (this is correct under the quasi-static approximation).

The implemented median and sciatic nerve models have respectively 28 and 37 fascicles, each populated with several neuronal populations. It is computationally inefficient to compute the response of all the fascicles within the nerve for each AS injecting current. Instead only the fascicles close to the activated contact have to be considered for computation, since it is impossible to affect the further ones without first soliciting the sensations conveyed by the closer ones.

A series of simulations were executed in order to establish an effective range of fascicles to compute, for each stimulating AS. Simulations showed that no fibers are being activated selectively 2000 μm away from the current source, in any configuration. Therefore, a fascicle

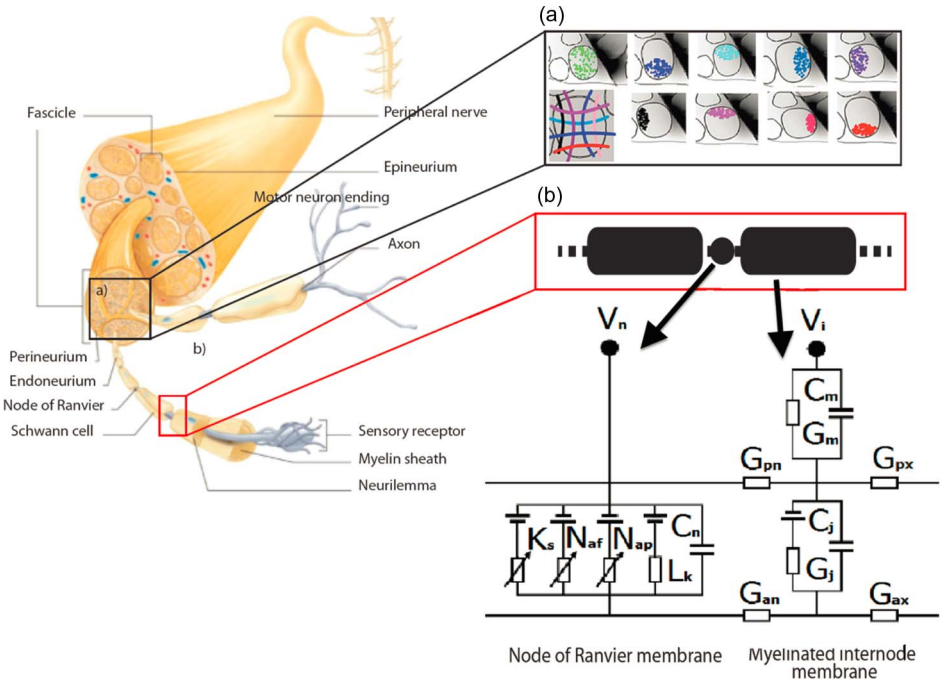

Fig. 3. ***Hybrid computational model of peripheral nerve: Since the positioning of the population of fibers of interest is unknown, these are simulated in different possible positions and extensions over the fascicle, represented in different colors, emulating the anatomical variability (a). Different nerve structures are implemented in corresponding compartments of the model (b). The nerve schematic on the left is adapted from http://www.allwidewallpapers.com/nerve-peripherax/bmVydmUtcGVyaXBoZXJheA.***

is computed when one of its fibers was within 2000 μm from the AS that is injecting current. By limiting in this way the simulations executed, the overall calculation power needed is drastically reduced.

III. MODELS IN PRACTICE: PROSTHESES WITH SENSORY FEEDBACK FOR UPPER AND LOWER LIMBS

In continuation, the models are exploited for electrodes design, development of protocols of stimulation, and for understanding and interpreting stimuli effects.

A. Indexes for Evaluation of the Prostheses With Sensory Feedback

In order to objectively evaluate the performance of the devices, the definition of appropriate selectivity indexes is essential. These will be used for tuning a device design toward the optimized solution. While it is straightforward for the case of motor neuroprostheses (the outcome is observable, and easily possible to evaluate by means of muscular recruitment curves), it is not trivial to define an appropriate measure for sensory fibers stimulation. The first selectivity index (taken from [19]) measures the percentage of fibers activated in a specific fascicle without recruiting the others.

It evaluates the spatial selectivity and is formulated as

$$\mathrm{Sel}_i = \mu_i - \frac{1}{m-1}\sum_{j=1, j\neq i}^{m} \mu_j \tag{4}$$

where μ_i is the percentage of recruitment defined as a number of axons activated by means of extracellular

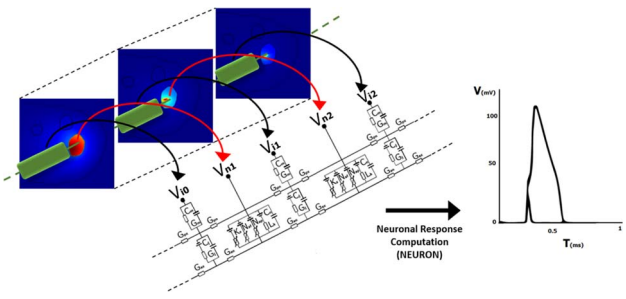

Fig. 4. ***Merging of FEM and NEURON models: The results of voltage distribution (on the left, in 3-D prospective) are exported from FEM and interpolated to the positions corresponding to the relevant parts of neuronal structure (circuit on the right). Then the value is modulated by simple multiplication until the value of extracellular voltage, for which the threshold is reached and the spike is elicited.***

voltage, divided by the total number of axons in the *i*th fascicle.

On the other hand, since the activation of a single fiber can trigger a perception [60], taking this into the account, a second selectivity index was proposed as follows:

$$\mathrm{Sel}_s = \frac{n_i}{\sum_{j=1}^{m} n_j} \tag{5}$$

where n_i is the number of axons activated by extracellular voltage in the *i*th fascicle. This index evaluates the functional selectivity. For all the modeled configurations of stimulation, a number of individual fascicles selectively recruited were computed by means of both indexes. The current amplitude at which 10% of fibers within the fascicle were activated represents the threshold [19].

B. Models Used for Optimal Design of Electrodes and Protocols of Stimulation

1) Electrode Geometry: The first, straightforward use of models is to understand which type of electrode geometry is the most prominent one for a selective elicitation of discrete sensations. To reach this goal, we implemented models of two electrodes (Fig. 5), which were successfully used in human sensory feedback restoration: TIME [6] and FINE [7]. Intraneural electrodes ensure smaller distance to their neural target than epineural electrodes. To compare their outcomes, we implemented a TIME with 14 ASs and two grounds, 0.4 mm of interdistance between ASs, 4 mm of total length, and 2.4 mm of effective length (that is the distance between the first and last AS). The diameter of AS was 80 μm [6], [34] and material properties as in [32]. To properly compare the two cases, the FINE electrode included 14 ASs. Contact stimulation surface was 0.25 mm $\times$ 0.25 mm. The height, width, and depth of the entire structure were 2.5, 4.7, and 7 mm, respectively, and material properties were taken from [18]. The results indicate that the most striking advantage of using the TIME is the possibility to selectively stimulate deep target fascicles (green crosses in Fig. 5), while this result is not achievable by using an epineural electrode. Moreover, the charge threshold needed to elicit fibers responses with TIME is one-order-of-magnitude lower compared to the case of the FINE electrode. Finally, the model indicates that it is possible to fine-tune the sensation through the gradual eliciting of the axonal response by simple charge modulation by a TIME AS; however, the same outcome cannot be achieved with FINE electrodes. Similar results were found in the experimental studies [6], [7], [30], [34].

2) Electrodes Dimensioning: Appropriate electrode dimensions, the number of ASs, and their interdistance are essential for the manufacturing process. The sciatic nerve

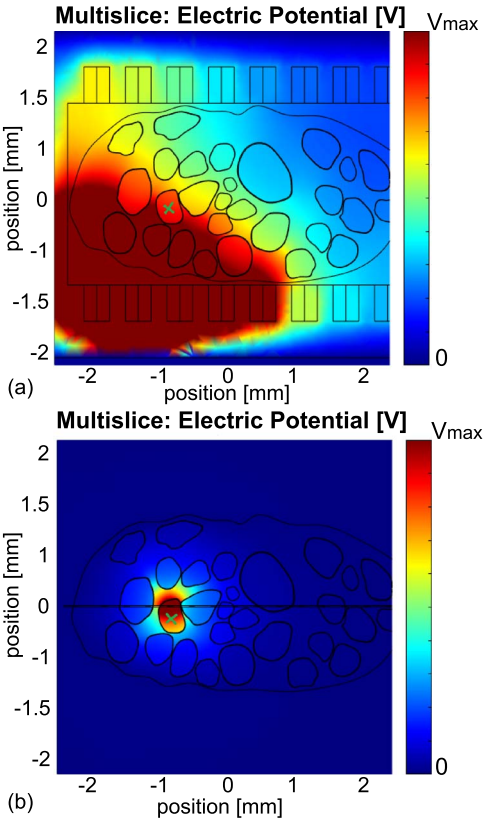

Fig. 5. ***Importance of the electrode geometry for the efficacy of the prosthetic device. The target fascicle (green X) is selectively stimulated by means of the TIME (a) while it cannot be exclusively stimulated by means of the FINE, without first stimulating the more superficial ones (b). The elicited voltage distributions are plotted in the planes orthogonal to centers of stimulating AS.***

with implanted TIMEs and potential distributions for selectively recruited fascicles are shown in Fig. 6.

The length of the electrode was designed in compliance with the dimensions of the nerve (18.75 mm larger diameter) to potentially reach all the fascicles. The ASs were spread evenly on both sides of its insulating substrate, which is 20 μm thick [32]. All the electrical parameters were taken from [19], [32], and [34]. TIME models with 8, 12, 16, 20, 24, and 28 ASs were created to determine the optimal number of contacts per electrode; three of these configurations are shown in Fig. 6. Their respective widths are 360, 580, and 800 μm: this dimension changes since more conducting leads are needed for a higher number of ASs. Our simulations showed that the model of TIME with 12 ASs was selectively stimulating six fascicles, while TIME with 20 contacts simulated nine fascicles. This represents almost 50% higher effectiveness of the electrode design by only eight extra AS implementations.

The further increase in the number of ASs does not yield significant improvement to the electrode

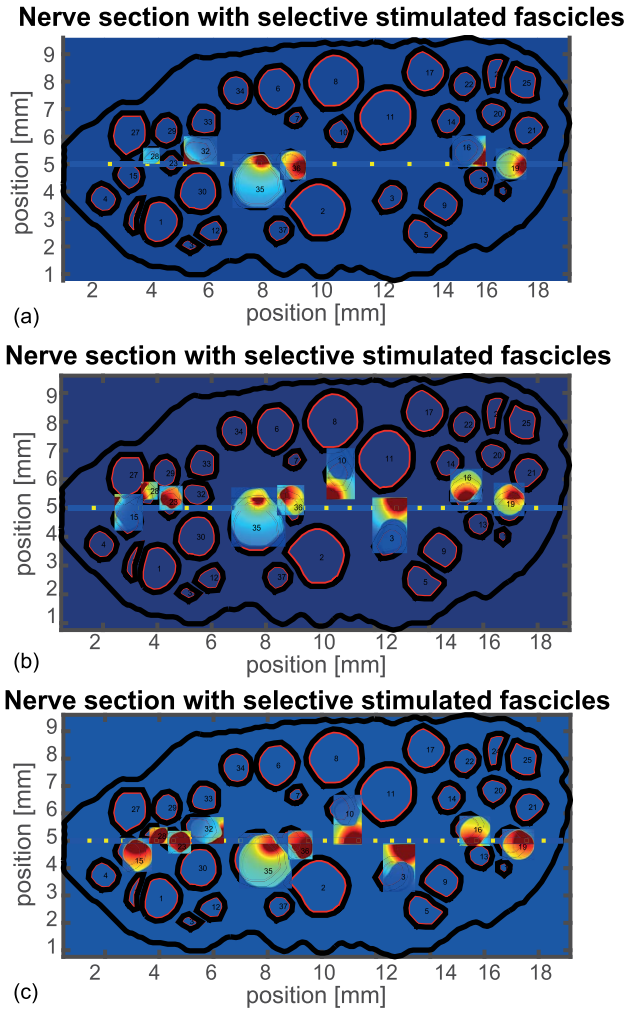

Fig. 6. ***Optimal electrode dimensioning: TIME models with 12, 20, and 28 ASs are represented in (a), (b), and (c). Highlighted insets represent the fascicles selectively stimulated. The elicited voltage distributions are plotted in the planes orthogonal to the center of stimulating AS. While the increase from 12 to 20 ASs yields a significant augmentation in the number of selectively stimulated fascicles, it becomes marginal as the number of ASs implemented reaches 28.***

performance. Indeed, a model with 28 contacts provides ten fascicles selectively recruited (11% gain). The total number of selectively stimulated fascicles is correlated with the number of ASs, but some of them are recruited selectively by more than a single AS. When dealing with a high number of ASs, there is a limiting factor due to the presence of leads, necessary to connect the device to the stimulator. When the number of contacts rises, the number of leads increases, thus the neural interface results in being bulkier and therefore more invasive.

3) Optimal Number of Implants: Neurosurgery Guidelines: In order to achieve the maximal performance during the stimulation (defined as the maximal possible number of fascicles selectively recruited), combined with limited nerve damage, it is crucial to understand the optimal number of electrodes to implant. Technically, an implantation of many electrodes can be useful to stimulate every fascicle within the nerve. However, too many electrodes could damage the nerve, and put excessive demand on the implantable electronics and transcutaneous communication implementation. Hence, the outcome of a computer model becomes of essential value for the neurosurgeon. The models of human median nerve with 1, 2, and 3 TIMEs inserted along the nerve larger diameter are implemented. The simulated dimensions are corresponding to those of a TIME with 14 ASs, as detailed in Section III-B1, while the electrical parameters are those of the original TIME [19], [34]. The simulations results (see Fig. 7) show that the selectivity during stimulation strongly increases, by passing from one electrode (positioned in the middle of the nerve) to two electrodes implanted in parallel (one above the other). When three TIMEs are implemented [Fig. 7(c)], the stimulation performance slightly increases, thus not justifying the third implant.

Comparing the number of fascicles selectively recruited by the stimulation, the setup using two TIMEs implanted, inserted parallel to the larger diameter of the nerve, results in an optimal coverage of fascicles with respect to the number of devices to implant. In fact, Fig. 7 shows that a single TIME with 14 ASs is selectively stimulating five different fascicles, but two devices in parallel are able to stimulate 12 different fascicles. By adding another electrode to the nerve, the number of fascicles elicited increases to 16, so only four fascicles more than with two electrodes.

This indicates that the marginal benefits of the configuration with three electrodes do not outweigh the damages occurring with an insertion of the extra device.

4) Design of Optimal Protocols for Stimulation: Monopolar stimulation consists in the activation of only one AS at the time, whereas multipolar protocols foresee the use of two or more contacts in any configuration (with opposite or the same phase of injected current) [61]. TIME and FINE implants, with 32 ASs each, and the geometrical and electrical properties as described above were implemented in the sciatic nerve (see Fig. 8). The potential distribution for monopolar [Fig. 8(a)] and bipolar stimulation with different polarities [Fig. 8(b)], and respective fascicle recruitments [Fig. 8(c) and (d)] were computed. The monopolar stimulation through AS9 [voltage distribution in Fig. 8(a)] did not allow for a selective activation of any fascicle. This can be seen in Fig. 8(c) where fascicles 25 and 24 are simultaneously recruited, applying the same charge.

By use of bipolar stimulation, it is possible to simultaneously apply the opposite currents to the adjoining AS10 resulting in the voltage distribution shown in Fig. 8(b).

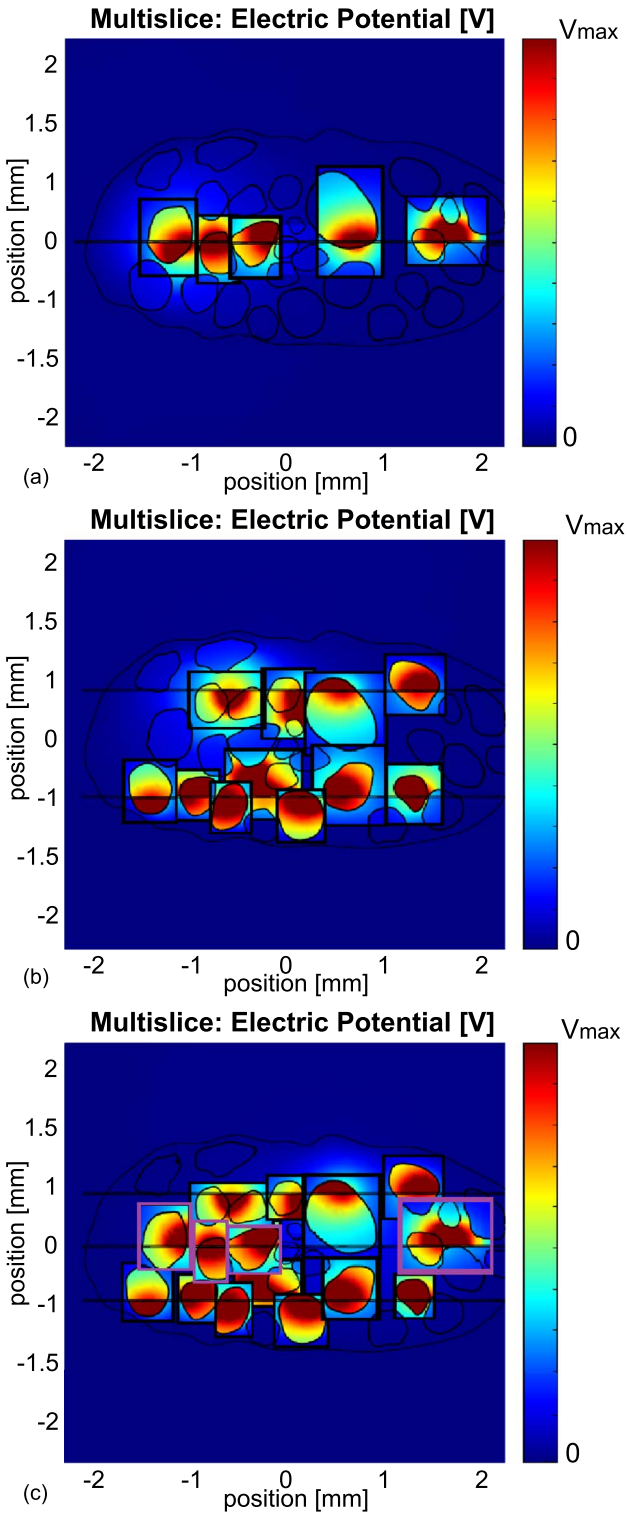

Fig. 7. ***Neurosurgical planning of median nerve implantation: determination of the optimal number of implants. Implants of 1, 2, and 3 TIMEs are presented in (a), (b), and (c). Highlighted insets represent the fascicles selectively stimulated, together with the voltage distribution in the most depolarized plane for specific ASs. When using one device, five fascicles (a), with two devices, 11 fascicles (b), with three devices, only four more fascicles (pink squares) (c) are selectively stimulated.***

This suppressed the spread of current from AS9 and therefore there was no activation of fibers in fascicle 24 resulting in the selective recruitment of the targeted fascicle 25 [see Fig. 8(d)].

These representative examples clearly display the potential improvements of the stimulation protocol design, guided by the model results. If the sensation in the third finger was conveyed by means of a fascicle targetable only with bipolar stimulation, this would have enabled an otherwise unmet functionality. In Fig. 8(e) and (f), a similar enhancement of device functionality can be seen for both TIME and FINE, respectively. The fascicles of sciatic nerve selectively elicited by monopolar protocol are represented in green, while in yellow are the ones that can be gained through the use of bipolar stimulation. More sophisticated policies of stimulation, such as the promising approach using pulsewidth modulation, presented in [7], should be tested in the future. Appropriate models will provide correct interpretation of their potential impact.

C. Use of Models to Understand the Mechanisms Involved in Neuroprosthesis

The presented modeling framework can be further exploited for the interpretation and investigation of scientific questions, which are difficult, or even impossible to solve, using an empirical approach.

As a striking example of sophisticated use of neuroprostheses in innovative bionic hands, we recently showed that texture discrimination could be artificially provided in human subjects by implementing a neuromorphic real-time mechanoneurotransduction (MNT) stimulation of cutaneous afferents [34]. We achieved these outcomes through temporal pattern modulation of electrical pulses delivered to the human median nerve via percutaneous microneurography stimulation in four healthy subjects and via implanted TIME stimulation in one transradial amputee. In this study, the use of model of the human median nerve had a pivotal role: indeed we first tested and tuned the model in four healthy subjects, by means of microneurographic needle stimulation. Then, we proved, by modeling simulations (Fig. 9), that the electrical fields produced by the microneurographic tips and TIME ASs are comparable.

Three types of positioning are typical representation for intraneural stimulating electrodes devices: in order to be able to selectively stimulate a specific fascicle (and therefore to elicit a sensation), the AS has to be within the fascicle of interest, or close to it. An eventual third case is when the intermediate untargeted fascicle is between the AS and the fascicle of interest, which could convey a sensation, which is not target for our prosthesis.

In particular, we tested if the thresholds are similar for the simulation of axonal populations with the TIME AS and microneurographic tips, in three categories of positioning with respect to the fascicle of interest: inside the fascicle, in proximity of the fascicle (outside a

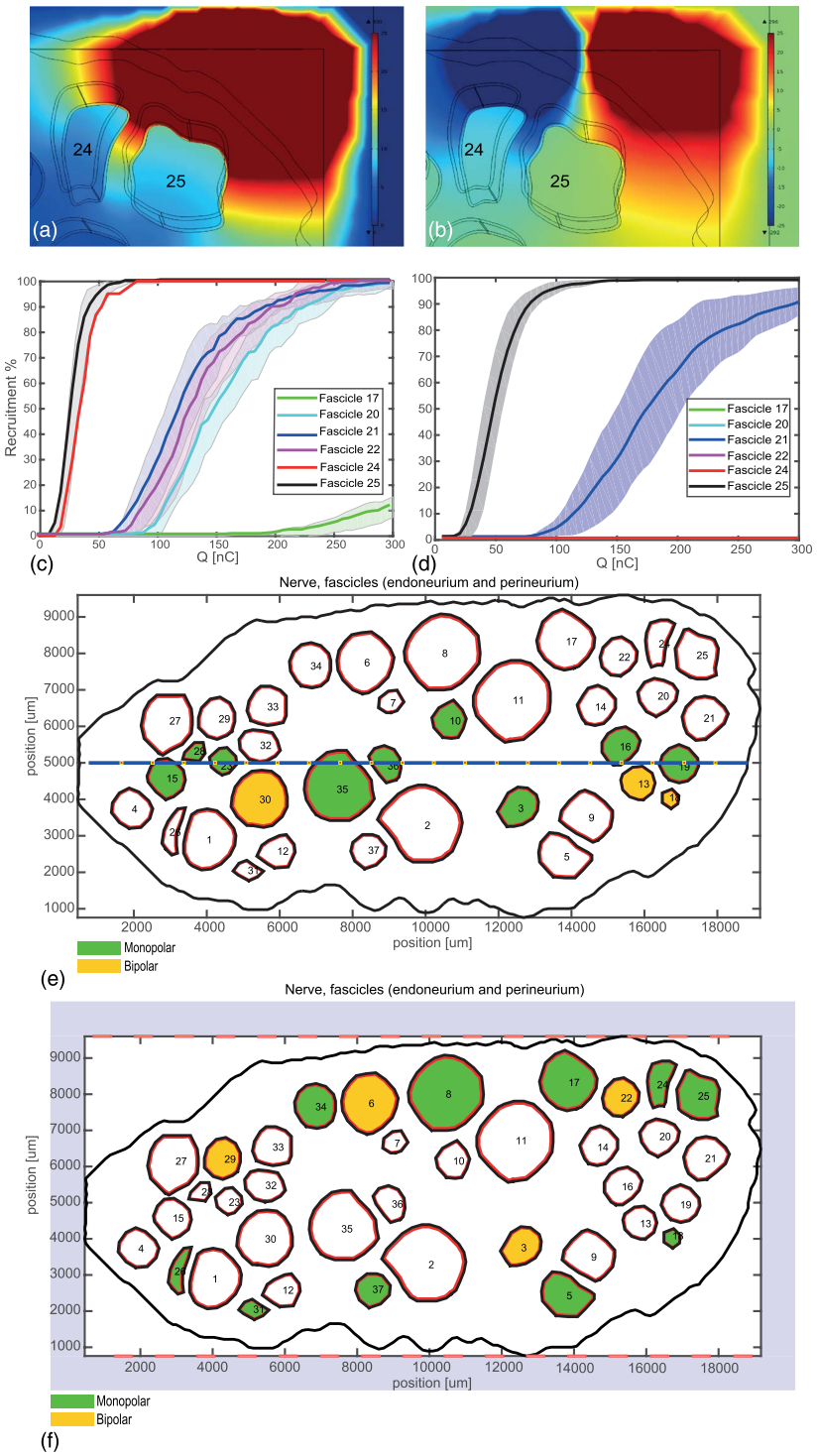

Fig. 8. ***Bipolar stimulation enhances the functionality of interface with respect to monopolar use. Voltage distribution elicited by AS9 monopolar stimulation (a) and AS9 and AS10 bipolar stimulation (b) are computed. The recruitments of underlying fascicles are shown in (c) and (d) for monopolar and bipolar stimulation, respectively. Several new fascicles are selectively elicited by bipolar stimulation (in yellow) with respect to monopolar (green), for both TIME (e) and FINE (f).***

fascicle, close to it), or shielded (outside a fascicle, with another fascicle in the middle, acting as a "shield").

Results showed that the thresholds for recruitment in corresponding placements were not statistically different, and therefore justified the use of the paradigm tested in healthy subjects, in amputees with an implantable device. These outcomes have also a wider scientific relevance: if successfully tested by minimally invasive

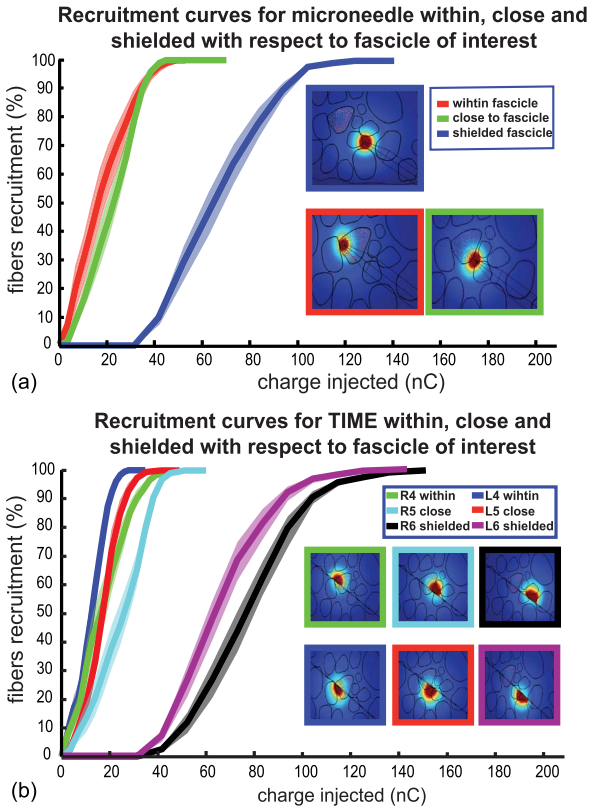

Fig. 9. ***Translation from acute to chronic preparation: Microstimulation is a useful experimental preparation for sequent implantable devices use. Median nerve stimulation by means of microneurographic needle (a) indicates similar field and axonal recruitment results as the TIME (b), when they are placed in the same positions (within the targeted fascicle, close to it, and shielded with other fascicle in the middle with respect to it). Axonal recruitments are computed for the voltages represented in the insets, with the respective color coding. Taken from [30] with permission.***

microneurographic preparation, and properly tuned, encoding strategies for human afferents stimulation can be translated to implantable solutions.

One of the biggest issues with long-term use of neural interfaces is the decay/change of the stimulating ability over time [41], [42], [62]–[65]. Even though a significant amount of studies has been performed [62]–[65], the mechanisms behind threshold's increase during chronic neural stimulation are not yet elucidated. Among many possible interpretations there is no scientific consensus. Several plausible hypotheses, which aim to explain the change of charge necessary to stimulate the nerve over time, were tested (see Fig. 10). We computed the elicited axonal population responses, when:

1) the electric field is perturbed by the fibrotic tissue, which has different electrical properties with respect to the nerve [20];
2) nerve fibers die after the AS is placed intrafascicularly;
3) fibrotic tissue pushes the AS away from the nerve fibers when placed intrafascicularly;
4) fibrotic tissue shifts the AS away from the fascicle when placed extrafascicularly.

Assumptions about relevant positioning are similar to those explicated in Fig. 9. The third case (shielded stimulation), where the AS stimulates the untargeted fascicle, and therefore elicits unwanted sensation, is not relevant to the present analysis.

To model a fibrotic growth over the electrode we implemented a rectangular sandwich, with varying thickness of [0 25 50 75 100 150 200] μm and static width and height of 150 μm [9], [62]–[65]. The thickness variation is implemented to emulate the fibrotic tissue increase during the weeks after the implantation. We set the conductivity of this tissue to 0.1 S/m, which is in the range stated by previous studies [20], [62]–[65]. First, we observed that the conductivity change does not influence axonal responses, similarly as shown in DBS modeling [20].

Our results indicate that cellular death probably is not the mechanism that induces threshold change. In this case [Fig. 10(b)], indeed, it would be impossible to elicit the full range of a sensation, but rather just part of it. Moreover, the threshold would be similar over time, as it can be observed by inspecting the value of charge necessary to elicit the 10% of full recruitment. This does not happen during long-term experiments [6]. When the axonal displacement is implemented [Fig. 10(a)], fiber recruitment occurs over the whole range of recruitment (and therefore of elicited sensation). It has very low stimulation threshold and is not affected by fibrosis growth. This situation corresponds to the one observed in [6] for the ulnar AS used for the prosthesis control. Finally, in the case of an AS placed outside, but in proximity to a fascicle of interest, results indicate a very interesting outcome [Fig. 10(c)]. Indeed the shift of the AS, resulting from the tissue growth, augments the threshold values, similarly to what we observed for the median nerve AS, used in [6] for the bidirectional prosthesis control. These results, together with experimental ones, promote the importance of intrafascicular implantation of ASs. This will assure lower thresholds and more stability of device functionality over time.

IV. DISCUSSION AND CONCLUSIONS

The framework for the design of neuroprostheses based on the deep understanding of underlying physics is a "hypothesis-driven" approach, in sharp contrast with the often-wise used "curiosity-driven" one. It enables to perform the most efficient manufacturing, avoid unnecessary animal experimentation, reduce costs, gain insight into unexpected phenomena, and finally propose guidelines for neurosurgical procedures.

It is of paramount importance to understand that models can be used properly only when addressing a

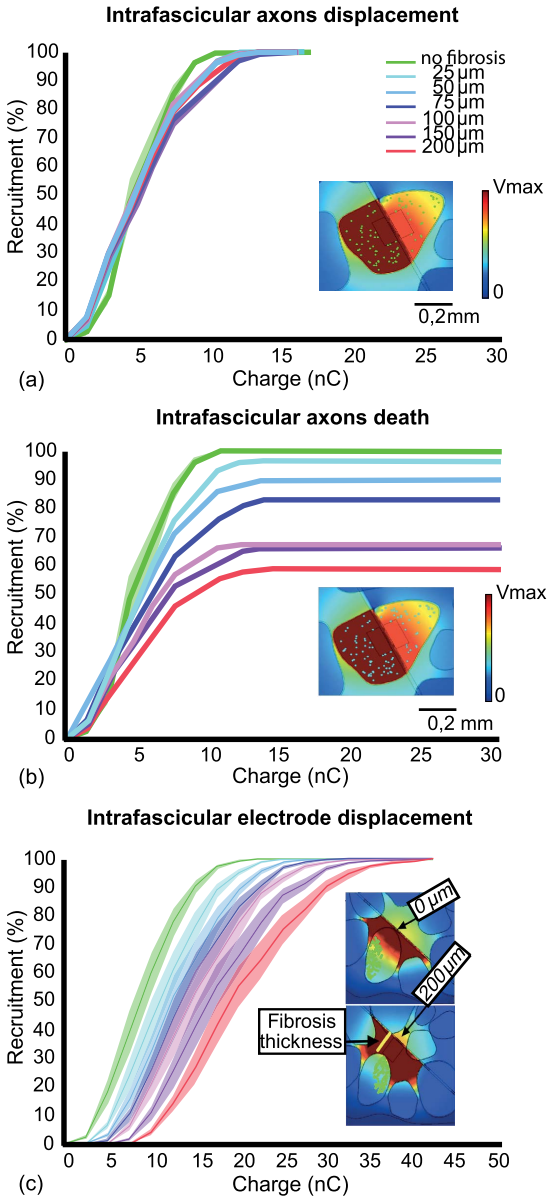

Fig. 10. ***Modeling interpretation of threshold changing over time. Three possible hypotheses were tested: axons displacement due to the fibrosis when the active site is intrafascicular (a), axons death in the area of the fibrosis, when the active site is intrafascicular (b), and displacement of the active site away from the fascicle, due to the fibrosis growth, when it is placed outside the fascicle itself (c). Computed recruitment curves correspond in color to the thickness of the fibrosis as in (a).***

clearly defined issue, which they are tailored for: models cannot be intended to explain all the aspects of such a complex system as neural system stimulation in its every aspect. Therefore, models have to be customized in compliance with the peculiar application or feature of interest.

In this study, results concerning the understanding of effects, which are computed for a general fascicle, are potentially generalizable to any PNS nerve model. Such results are: 1) fibrotic answer; 2) microneedle device usability for predictions of the behavior of chronically implanted electrodes; and 3) bipolar stimulation. On the other side, the dimensions, geometry, the number of active sites of optimal neural interface are nerve-section dependent. In order to overcome this nerve-section anatomy dependence, it is of great importance to gather a better understanding of the nerve topography with respect to their innervations. To this end recent anatomical studies are done in cadaveric preparations of median [66] and sciatic nerve [67], revisiting the traditional Sunderland's work [68]. However, they mainly investigated distal topography, while on the proximal level, which is of our interest, the information is yet partial. Future studies are needed to further our knowledge of the nerve topography on the proximal level.

An important aspect of modeling is the experimental validation of the simulations results. Some parameters are difficult to find or measure, and therefore they need to be extrapolated from the existing measurements, which are usually done for different mammalian species. In these cases, experiments can help to unveil if the set of assumed parameters is properly selected for the particular model exploitation. Experimental measurements performed for validation must be carefully designed, so to choose the output measure, often macroscopic, which is meaningful for the particular system, which is, by its nature, microscopic. For the great majority of models implemented in the field of motor neuroprosthetics, choosing the output measurements is straightforward: in the case of the rat sciatic nerve model stimulated with TIME, the muscular signals were measured [30], [35], while in the model of spinal cord stimulation, the simple reflex measurements were used for confirming the role of afferents in the EES [23]. Such a task is much more complicated in the case of feedback-restoring prostheses. We showed that the use of minimally invasive techniques (e.g., microneurography) is a promising practice [34] to use in order to validate the models and exploit them for future predictions with the chronically implanted interfaces. The range of charge necessary for the recruitment and thresholds observed during the TIME simulations in this study are similar to the ones observed in the human experiments [6]. Particularly, in Fig. 10, we showed two examples of active site placements, which are emulating the two active sites used for bidirectional control in [6].

Every model comes with specific limitations, and these should be clearly studied and stated, since they could help in the correct interpretation of model results, their future exploitation, and upgrading. In this work, among several issues, the main limit is the lack of the electrode–electrolyte interface [69]. Moreover, in both models, we assume that a single fascicle conveys a single type of sensation, for the discrete and

concentrated innervation area of a hand or a foot. This is, however, a reasonable assumption, based on literature data [45], [59].

At the same pace of development of innovative models, it is essential to work on their optimization, so that they can be used for the exploration of a huge space of parameters, by future heuristic algorithms.

We believe that, thanks to the future technological development, especially of imaging techniques, the sophisticated and widespread neuroprosthetic devices will go toward the customized modeling-based approach. Starting from the high detailed images of the structure of interest, and anatomical knowledge, by the use of powerful computers, and efficient modeling computation, we could create the patient-specific neural interfaces and protocols of use.

In this work, we have shown the models of a human median and sciatic nerve, which resulted in finding of the optimal dimensions of devices to use. This includes shape, the number of ASs, and their placements, for the specific nerve sections. The model indicates that bipolar stimulation is promising to enable the eliciting of areas of hand and foot, eventually relevant for the successful bidirectional control, and not possible to recruit by single-channel stimulation.

An important guideline on the optimal number of implants per nerve has been provided: this is useful for neurosurgery planning and for the implantable electronics design. Indeed by augmenting the number of devices, and therefore of ASs, the problems, concerning the connection of these to implantable neurostimulator, arise together with an augmented power and data transmission requirements. Our model indicated two TIME devices as the optimal number of implants for median nerve; this corresponds to our study with an amputee [6], where indeed two implants per nerve produced excellent results.

Models indicated the possibility to use the acute microneedle preparation for tests and validation of innovative stimulation strategies, before their employment within the implanted device.

Finally, we provided indications on the possible reasons for the threshold variation during time. Such a behavior is due to the displacement of ASs placed outside the fascicle, and not for those being intrafascicular. This provides a useful guide for the design of future devices, which should be tailored for the intrafaciscular AS placement.

Feedback restoration enabled upper limb amputees to feel touch sensations from the missing hand, to exploit them in prosthesis bidirectional control, and to diminish their phantom pain [6], [7], [70].

By an innovative biomimetic electrical stimulation of residual sciatic nerve with optimally designed and implanted device, natural sensations will be elicited from amputee's missing feet. These sensations have a pivotal role in the correct balance and walking [59], [71]. The use of sciatic nerve stimulation for the sensory restoration in lower limb amputees, or nerve-injured, will potentially enable the reestablishment of the correct sensory-motor scheme. This will induce fall prevention, ameliorate walking dynamics, diminish metabolic cost and phantom limb pain level, and boost the prosthesis embodiment, which are among the biggest problems encountered [71]. Both of these interventions, perfected by computer models, will potentially help the natural and intuitive brain-sensory-motor reintegration, which will enable the CNS to automatically adjust and accept the use of the artificial prosthesis, improving the health and quality of life of the disabled people. ■

REFERENCES

[1] J. A. Obeso *et al.*, "Deep-brain stimulation of the subthalamic nucleus or the pars interna of the globus pallidus in Parkinson's disease," *New England J. Med.*, vol. 345, pp. 956–963, 2001.

[2] M. S. Humayun *et al.*, "Visual perception in a blind subject with a chronic microelectronic retinal prosthesis," *Vis. Res.*, vol. 43, no. 24, pp. 2573–2581, 2003.

[3] P. C. Loizou, "Introduction to cochlear implants," *IEEE Eng. Med. Biol. Mag.*, vol. 18, no. 1, pp. 32–42, 1999.

[4] C. A. Angeli, V. R. Edgerton, Y. P. Gerasimenko, and S. J. Harkema, "Altering spinal cord excitability enables voluntary movements after chronic complete paralysis in humans," *Brain*, vol. 137, pp. 1394–1409, 2014.

[5] R. B. North, D. H. Kidd, M. Zahurak, C. S. James, and D. M. Long, "Spinal cord stimulation for chronic, intractable pain: Experience over two decades," *Neurosurgery*, vol. 32, no. 3, pp. 384–395, 1993.

[6] S. Raspopovic *et al.*, "Restoring natural sensory feedback in real-time bidirectional hand prostheses," *Sci. Transl. Med.*, vol. 6, 2014, Art. no. 222ra19.

[7] D. W. Tan *et al.*, "A neural interface provides long-term stable natural touch perception," *Sci. Transl. Med.*, vol. 6, 2014, Art. no. 257ra138.

[8] X. Navarro *et al.*, "A critical review of interfaces with the peripheral nervous system for the control of neuroprostheses and hybrid bionic systems," *J. Peripher. Nerv. Syst.*, vol. 10, pp. 229–258, 2005.

[9] N. Lago, K. Yoshida, K. P. Koch, and X. Navarro, "Assessment of biocompatibility of chronically implanted polyimide and platinum intrafascicular electrodes," *IEEE Trans. Biomed. Eng.*, vol. 54, no. 2, pp. 281–290, 2007.

[10] C. C. McIntyre and W. M. Grill, "Finite element analysis of the current-density and electric field generated by metal microelectrodes," *Ann. Biomed. Eng.*, vol. 29, no. 3, pp. 227–235, 2001.

[11] D. R. Merrill, M. Bikson, and J. G. R. Jefferys, "Electrical stimulation of excitable tissue: Design of efficacious and safe protocols," *J. Neurosci. Methods*, vol. 141, pp. 171–198, 2005.

[12] D. R. McNeal, "Analysis of a model for excitation of myelinated nerve," *IEEE Trans. Biomed. Eng.*, no. 4, pp. 329–337, 1976.

[13] F. Rattay, "Analysis of models for external stimulation of axons," *IEEE Trans. Biomed. Eng.*, no. 10, pp. 974–977, 1986.

[14] F. Rattay, "Analysis of models for extracellular fiber stimulation," *IEEE Trans. Biomed. Eng.*, vol. 36, no. 7, pp. 676–682, 1989.

[15] C. M. Zierhofer, "Analysis of a linear model for electrical stimulation of axons-critical remarks on the 'activating function concept'," *IEEE Trans. Biomed. Eng.*, vol. 48, no. 2, pp. 173–184, 2001.

[16] M. A. Moffitt, C. C. Mcintyre, and W. M. Grill, "Prediction of myelinated nerve fiber stimulation thresholds: Limitations of linear models," *IEEE Trans. Biomed. Eng.*, vol. 51, no. 2, pp. 229–236, 2004.

[17] C. C. McIntyre and W. M. Grill, "Extracellular stimulation of central neurons: Influence of stimulus waveform and frequency on neuronal output," *J. Neurophysiol.*, vol. 88, no. 4, pp. 1592–1604, 2002.

[18] M. A. Schiefer, R. J. Triolo, and D. J. Tyler, "A model of selective activation of the femoral nerve with a flat interface

nerve electrode for a lower extremity neuroprosthesis," *IEEE Trans. Neural Syst. Rehabil. Eng.*, vol. 16, no. 2, pp. 195–204, 2008.

[19] S. Raspopovic, M. Capogrosso, and S. Micera, "A computational model for the stimulation of rat sciatic nerve using a transverse intrafascicular multichannel electrode," *IEEE Trans. Neural Syst. Rehabil. Eng.*, vol. 19, pp. 333–344, 2011.

[20] S. Miocinovic *et al.*, "Computational analysis of subthalamic nucleus and lenticular fasciculus activation during therapeutic deep brain stimulation," *J. Neurophysiol.*, vol. 96, no. 3, pp. 1569–1580, 2006.

[21] A. M. Frankemolle *et al.*, "Reversing cognitive-motor impairments in Parkinson's disease patients using a computational modeling approach to deep brain stimulation programming," *Brain*, vol. 133, no. 3, pp. 746–761, 2010.

[22] E. M. Moraud *et al.*, "Mechanisms underlying the neuromodulation of spinal circuits for correcting gait and balance deficits after spinal cord injury," *Neuron*, vol. 89, pp. 814–828, 2016.

[23] M. Capogrosso *et al.*, "A computational model for epidural electrical stimulation of spinal sensorimotor circuits," *J. Neurosci.*, vol. 33, pp. 19326–19340, 2013.

[24] F. Rattay, K. Minassian, and M. R. Dimitrijevic, "Epidural electrical stimulation of posterior structures of the human lumbosacral cord: 2. Quantitative analysis by computer modeling," *Spinal Cord*, vol. 38, pp. 473–489, 2000.

[25] A. G. Richardson, C. C. McIntyre, and W. M. Grill, "Modelling the effects of electric fields on nerve fibres: Influence of the myelin sheath," *Med. Biol. Eng. Comput.*, vol. 38, no. 4, pp. 438–446, 2000.

[26] C. C. McIntyre, A. G. Richardson, and W. M. Grill, "Modeling the excitability of mammalian nerve fibers: Influence of afterpotentials on the recovery cycle," *J. Neurophysiol.*, vol. 87, no. 2, pp. 995–1006, 2002.

[27] M. L. Hines and N. T. Carnevale, "The neuron simulation environment," *Neural Comput.*, vol. 9, no. 6, pp. 1179–1209, Aug. 1997.

[28] B. Coburn and W. K. Sin, "A theoretical study of epidural electrical stimulation of the spinal cord—Part I: Finite element analysis of stimulus fields," *IEEE Trans. Biomed. Eng.*, no. 11, pp. 971–977, 1985.

[29] B. Coburn, "A theoretical study of epidural electrical stimulation of the spinal cord—Part II: Effects on long myelinated fibers," *IEEE Trans. Biomed. Eng.*, no. 11, pp. 978–986, 1985.

[30] S. Raspopovic *et al.*, "Experimental validation of a hybrid computational model for selective stimulation using transverse intrafascicular multichannel electrodes," *IEEE Trans. Neural Syst. Rehabil. Eng.*, vol. 20, p. 395–404, 2012.

[31] G. G. Naples, J. T. Mortimer, A. Scheiner, and J. D. Sweeney, "A spiral nerve cuff electrode for peripheral nerve stimulation," *IEEE Trans. Biomed. Eng.*, vol. 35, no. 11, pp. 905–916, 1988.

[32] T. Boretius *et al.*, "A transverse intrafascicular multichannel electrode (time) to interface with the peripheral nerve," *Biosens. Bioelectron.*, vol. 26, pp. 62–69, 2010.

[33] A. Cutrone *et al.*, "A three-dimensional self-opening intraneural peripheral interface (SELINE)," *J. Neural Eng.*, vol. 12, no. 1, 2015, Art. no. 016016.

[34] C. M. Oddo *et al.*, "Intraneural stimulation elicits discrimination of textural features by artificial fingertip in intact and amputee humans," *Elife*, 2016, Art. no. e09148.

[35] J. Badia, D. Andreu, C. Azevedo-Coste, T. Stieglitz, and X. Navarro, "Comparative analysis of transverse intrafascicular multichannel, longitudinal intrafascicular and multipolar cuff electrodes for the selective stimulation of nerve fascicles," *J. Neural Eng.*, vol. 8, no. 3, 2011, p. 036023 (13).

[36] A. Vuckovic, J. M. Rijkhoff, and J. J. Struijk, "Different pulse shapes to obtain small fiber selective activation by anodal blocking-a simulation study," *IEEE Trans. Biomed. Eng.*, vol. 51, no. 5, pp. 698–706, 2004.

[37] W. M. Grill and J. T. Mortimer, "Stimulus waveforms for selective neural stimulation," *IEEE Eng. Med. Biol. Mag.*, vol. 14, no. 4, pp. 375–385, 1995.

[38] W. M. Grill and J. T. Mortimer, "Inversion of the current-distance relationship by transient depolarization," *IEEE Trans. Biomed. Eng.*, vol. 44, no. 1, pp. 1–9, 1997.

[39] K. Hennings, L. Arendt-Nielsen, S. S. Christensen, and O. K. Andersen, "Selective activation of small-diameter motor fibres using exponentially rising waveforms: A theoretical study," *Med. Biol. Eng. Comput.*, vol. 43, no. 4, pp. 493–500, 2005.

[40] M. A. Schiefer, D. J. Tyler, and R. J. Triolo, "Probabilistic modeling of selective stimulation of the human sciatic nerve with a flat interface nerve electrode," *J. Comput. Neurosci.*, vol. 33, no. 1, pp. 179–190, 2012.

[41] B. D. Winslow and P. A. Tresco, "Quantitative analysis of the tissue response to chronically implanted microwire electrodes in rat cortex," *Biomaterials*, vol. 31, no. 7, pp. 1558–1567, 2010.

[42] X. Liu *et al.*, "Stability of the interface between neural tissue and chronically implanted intracortical microelectrodes," *IEEE Trans. Rehabil. Eng.*, vol. 7, no. 3, pp. 315–326, 1999.

[43] W. Girsch *et al.*, "Histological assessment of nerve lesions caused by epineurial electrode application in rat sciatic nerve," *J. Neurosurgery*, vol. 74, no. 4, pp. 636–642, 1991.

[44] G. C. McConnell *et al.*, "Implanted neural electrodes cause chronic, local inflammation that is correlated with local neurodegeneration," *J. Neural Eng.*, vol. 6, no. 5, 2009, Art. no. 056003.

[45] M. E. Jabaley, W. H. Wallace, and F. R. Heckler, "Internal topography of major nerves of the forearm and hand: A current view," *J. Hand Surgery*, vol. 5, no. 1, pp. 1–18, 1980.

[46] G. Fenzl and R. Zinnecker, "Topography of the sciatic nerve's fibres in regard of clinical use," *Anatomischer Anzeiger*, vol. 163, no. 2, pp. 107–110, 1986.

[47] A. Q. Choi, J. K. Cavanaugh, and D. M. Durand, "Selectivity of multiple-contact nerve cuff electrodes: A simulation analysis," *IEEE Trans. Biomed. Eng.*, vol. 48, no. 2, pp. 165–172, 2001.

[48] Z. Lertmanorat and D. M. Durand, "Extracellular voltage profile for reversing the recruitment order of peripheral nerve stimulation: A simulation study," *J. Neural Eng.*, vol. 1, no. 4, p. 202, 2004.

[49] C. A. Bossetti, M. J. Birdno, and W. M. Grill, "Analysis of the quasi-static approximation for calculating potentials generated by neural stimulation," *J. Neural Eng.*, vol. 5, no. 1, pp. 44–53, 2008.

[50] A. Weerasuriya, R. A. Spangler, S. I. Rapoport, and R. E. Taylor, "AC impedance of the perineurium of the frog sciatic nerve," *Biophys. J.*, vol. 46, pp. 167–174, 1984.

[51] Y. Grinberg, M. A. Schiefer, D. J. Tyler, and K. J. Gustafson, "Fascicular perineurium thickness, size, and position affect model predictions of neural excitation," *IEEE Trans. Neural Syst. Rehabil. Eng.*, vol. 16, no. 6, pp. 572–581, 2008.

[52] J. R. Schwarz and G. Eikhof, "Na currents and action potentials in rat myelinated nerve fibres at 20 and 37 degrees C," *Pflugers Arch.*, vol. 409, no. 6, pp. 569–577, 1987.

[53] P. H. Schimpf, C. Ramon, and J. Haueisen, "Dipole models for the EEG and MEG," *IEEE Trans. Biomed. Eng.*, vol. 49, no. 5, pp. 409–418, May 2002.

[54] A. L. Hodgkin and A. F. Huxley, "A quantitative description of the membrane current and its application to conduction and excitation in nerve," *J. Physiol.*, 1952, vol. 117, pp. 500–544.

[55] Å. B. Vallbo and R. Johansson, "Properties of cutaneous mechanoreceptors in the human hand related to touch sensation," *Human Neurobiol.*, vol. 3, no. 1, pp. 3–14, 1984.

[56] H. Torebjörk and J. L. Ochoa, "Specific sensations evoked by activity in single identified sensory units in man," *Acta Physiologica Scandinavica*, vol. 110, no. 4, pp. 445–447, 1980.

[57] H. S. Garven, F. W. Gairns, and G. Smith, "The nerve fiber populations of the nerves of the leg in chronic occlusive arterial disease in man," *Scottish Med. J.*, vol. 7, pp. 250–265, 1962.

[58] D. Purves *et al.*, "Neuroscience, Animation 5.3: Ionotropic and Metabolic Receptors," in *Neuroscience*, 5th ed. Sinauer Associates, 2012.

[59] P. Kennedy and J. Inglis, "Distribution and behaviour of glabrous cutaneous receptors in the human foot sole," *J. Physiol.*, vol. 538, pp. 995–1002, 2002.

[60] J. Van Hees and J. M. Gybels, "Pain related to single afferent c fibers from human skin," *Brain Res.*, vol. 48, pp. 397–400, 1972.

[61] C. Veraart, W. M. Grill, and J. T. Mortimer, "Selective control of muscle activation with a multipolar nerve cuff electrode," *IEEE Trans. Biomed. Eng.*, vol. 40, no. 7, pp. 640–653, 1993.

[62] W. M. Grill and J. T. Mortimer, "Neural and connective tissue response to long-term implantation of multiple contact nerve cuff electrodes," *J. Biomed. Mater. Res.*, vol. 50, no. 2, pp. 215–226, 2000.

[63] J. B. Leach, A. K. H. Achyuta, and S. K. Murthy, "Bridging the divide between neuroprosthetic design, tissue engineering and neurobiology," *Front. Neuroeng.*, vol. 2, 2009, p. 18.

[64] K. H. Polasek *et al.*, "Stimulation stability and selectivity of chronically implanted multicontact nerve cuff electrodes in the human upper extremity," *IEEE Trans. Neural Syst. Rehabil. Eng.*, vol. 17, no. 5, pp. 428–437, 2009.

[65] X. Huang, D. Nguyen, D. W. Greve, and M. M. Domach, "Simulation of microelectrode impedance changes due to cell growth," *IEEE Sensors J.*, vol. 4, no. 5, pp. 576–583, 2004.

[66] U. Planitzer *et al.*, "Median nerve fascicular anatomy as a basis for distal neural prostheses," *Ann. Anatomy*, vol. 196, no. 2–3, pp. 144–149, 2014.

[67] K. Gustafson, Y. Grinberg, S. Joseph, and R. J. Triolo, "Human distal sciatic nerve fascicular anatomy: Implications for ankle control using nerve-cuff electrodes," *J. Rehabil. Res. Dev.*, vol. 49, pp. 309–321, 2012.

[68] S. Sunderland, "The intraneural topography of the radial, median and ulnar nerves," *Brain*, vol. 68, pp. 511 243–511 298, 1945.

[69] D. R. Cantrell, S. Inayat, A. Taflove, R. S. Ruoff, and J. B. Troy, "Incorporation of the electrode-electrolyte interface into finite-element models of metal microelectrodes," *J. Neural Eng.*, vol. 5, no. 1, p. 54, 2007.

[70] P. M. Rossini *et al.*, "Double nerve intraneural interface implant on a human amputee for robotic hand control," *Clin. Neurophysiol.*, vol. 121, pp. 777–783, 2010.

[71] R. Gailey, K. Allen, J. Castles, J. Kucharik, and M. Roeder, "Review of secondary physical conditions associated with lower-limb amputation and long-term prosthesis use," *J. Rehabil. Res. Develop.*, vol. 45, no. 1, p. 15, 2008.

ABOUT THE AUTHORS

Stanisa Raspopovic received the M.S. degree in biomedical engineering from the University of Pisa, Pisa, Italy, in 2007 and the Ph.D. degree in biomedical robotics from the Scuola Superiore Sant' Anna, Pisa, Italy, in 2011.

During 2007 and 2009, he was a Visiting Researcher at the Universitat Autonoma Barcelona, Spain, performing *in vivo* experimentation with peripheral nerve electrodes, for stimulation and decoding. In 2010, he was at ETH Zurich, Switzerland, working with the electrical epidural stimulation for the spinal cord injury rehabilitation. Since 2012, he has been a Researcher at the Center for Neuroprosthetics, École polytechnique fédérale de Lausanne (EPFL), Lausanne, Switzerland. His research interests include: bidirectional prosthetic control for amputees-sensory feedback restoration in humans, hybrid modeling of electrical stimulation of nerves by electromagnetic (finite element methods) and biophysical (NEURON) models, neural control of the movement and sensorimotor integration, neural signals decoding for control, and sensory encoding in neuroprosthetics.

Francesco Maria Petrini received the B.S. and M.S. degrees in biomedical engineering from the University of Rome Tor Vergata, Rome, Italy, in 2008 and 2010, respectively and the Ph.D. degree in robotics and neural engineering from the Campus Bio-Medico University of Rome, Rome, Italy, in 2015.

He was a visiting student at Imperial College of London, London, U.K., in 2010 and at École polytechnique fédérale de Lausanne (EPFL), Lausanne, Switzerland, from 2013 to 2015. Since 2015, he has been a Postdoctoral Researcher in the Translational Neural Engineering lab, EPFL. His main research interests include motor and sensory peripheral nervous system, interfaces with the peripheral nervous system, decoding and encoding algorithms, modeling of the peripheral nervous system, and prosthetics.

Dr. Petrini is a member of the Society for Neuroscience and the Society for the Neural Control of Movement.

Marek Zelechowski received the B.S. degree in biomedical engineering from Warsaw University of Technology (WUT), Warsaw, Poland, in 2014 and M.S. degrees in biomedical engineering from Cranfield University, Cranfield, U.K., in 2015 and WUT in 2016.

He was a visiting student in the Translational Neural Engineering Lab at École polytechnique fédérale de Lausanne (EPFL), Lausanne, Switzerland, in 2015. His research area covers 3-D modeling of peripheral nervous system, design of PNS interfaces, motion-tracking systems for gait analysis, and wearable health monitoring devices design.

Giacomo Valle received the B.S. degree in biomedical engineering and the M.S. degree in bioengineering (*cum laude*) from the University of Genoa, Genova, Italy, in 2014 and 2016, respectively. He will soon start his Ph.D. work at the Scuola Superiore Sant'Anna, Pisa, Italy

He is currently in the Translational Neural Engineering Lab (TNE), École polytechnique fédérale de Lausanne (EPFL), Lausanne, Switzerland. His research interests are in neuroengineering and computational models: neuroprostheses in animal and human models for the peripheral stimulation of the nervous system in order to understand the neural control of movement, prostheses control, and the sensory feedback.